INSTITUTE OF FLUID-FLOW MACHINERY
POLISH ACADEMY OF SCIENCES

TRANSACTIONS OF THE INSTITUTE OF FLUID-FLOW MACHINERY

111

WYDAWNICTWO IMP PAN

GDAŃSK 2002

EDITORIAL AND PUBLISHING OFFICE

IFFM Publishers (Wydawnictwo IMP), Institute of Fluid Flow Machinery, Fiszera 14, 80-952 Gdańsk, Poland, Tel.: +48(58)3411271 ext. 141, Fax: +48(58)3416144, E-mail: esli@imp.gda.pl

Financial support of publication of this journal is provided by the State Committee for Scientific Research, Warsaw, Poland

Terms of subscription

Subscription order and payment should be directly sent to the Publishing Office

Warunki prenumeraty w Polsce

Wydawnictwo ukazuje się przeciętnie dwa lub trzy razy w roku. Cena numeru wynosi 20,- zł + 5,- zł koszty wysyłki. Zamówienia z określeniem okresu prenumeraty, nazwiskiem i adresem odbiorcy należy kierować bezpośrednio do Wydawcy (Wydawnictwo IMP, Instytut Maszyn Przepływowych PAN, ul. Gen. Fiszera 14, 80-952 Gdańsk). Osiągalne są również wydania poprzednie. Prenumerata jest również realizowana przez jednostki kolportażowe RUCH S.A. właściwe dla miejsca zamieszkania lub siedziby prenumeratora. W takim przypadku dostawa następuje w uzgodniony sposób.

ISSN 0079-3205

TRANSACTIONS OF THE INSTITUTE OF FLUID-FLOW MACHINERY
Appears since 1960

Aims and Scope

Transactions of the Institute of Fluid-Flow Machinery have primarily been established to publish papers from four disciplines represented at the Institute of Fluid-Flow Machinery of Polish Academy of Sciences, such as:

- Liquid flows in hydraulic machinery including exploitation problems,
- Gas and liquid flows with heat transport, particularly two-phase flows,
- Various aspects of development of plasma and laser engineering,
- Solid mechanics, machine mechanics including exploitation problems.

The periodical, where originally were published papers describing the research conducted at the Institute, has now appeared to be the place for publication of works by authors both from Poland and abroad. A traditional scope of topics has been preserved.

Only original and written in English works are published, which represent both theoretical and applied sciences. All papers are reviewed by two independent referees.

TRANSACTIONS OF THE INSTITUTE OF FLUID-FLOW MACHINERY

No. 111, 2002, 109-132

EUGENIUSZ IHNATOWICZ and MARIAN TRELA*

Investigations of instability of liquid jets emanating from nozzles into ambient air – Part I†

Institute of Fluid-Flow Machinery of PAS, Fiszera 14, 80-952 Gdańsk, Poland

Abstract

The paper presents the results of investigations of instability of liquid jets emanating from contoured nozzles into ambient air. The major attention has been paid to the measurements of the jet structure and the distance beyond which the jet lost its continuity and was broken into liquid droplets. Investigations have been conducted at various pressures of water in the nozzle and its three diameters. The results have been compared against available data from literature.

Keywords: Liquid jet; Jet structure

Nomenclature

D	–	nozzle diameter, mm
L	–	length, distance, m
p	–	water pressure, Pa
R	–	electric resistance, Ω
Re	–	Reynolds number, $\mathrm{Re} = \rho w D/\mu$
T	–	temperature, ^oC
μ	–	dynamic viscosity, kg/ms
σ	–	surface tension, N/m
t	–	time, s
U	–	voltage, V
V	–	volumetric flow rate of water, l/min
w	–	mean water velocity at nozzle outlet m/s
We	–	Weber number, $\mathrm{We} = \rho w^2 D/\sigma$
ρ	–	density, specific resistance

Subscripts

b, B	–	breakdown, Bendemann's orifice
bar	–	barometric
c	–	contoured orifice
g	–	gas
l	–	liquid
max, min	–	maximum, minimum

*Corresponding author. E-mail address: mtr@imp.gda.pl

†The paper was supported by the Polish State Committee for Scientific Research, Grant No 8T 10B 03713

c	–	contoured orifice	max, min	–	maximum, minimum
cr	–	critical	s	–	droplet, sharp edge orifice
i	–	beginning of the region	w	–	water
j	–	liquid jet	I, II, III	–	refers to regions I, II, III

1 Introduction

A phenomenon of liquid jet outflow from the nozzle (hole) to the gas environment (free jets) is present in numerous technical equipment. Such jets have application for example in cooling of hot surfaces, two-phase ejectors (water-steam, water-air), liquid sprays (burners, fuel injectors) and other technical cases. Such jets, at some distance from the nozzle, break up into droplets and a mixture of droplets and gas is being formed. In practical applications continuous jet cooling can be applied [1-3] or alternatively spray cooling [4]. Sufficient liquid atomisation into the form of small droplets (dispersed flow) as well as their correct mixing with gas decides about the efficiency of technical equipment utilising the latter form of cooling. In all mentioned above applications, apart from the quality of spraying, important also is the distance, after which the dispersed flow takes place. This is a very important parameter, and hence it should be of no surprise that it has been a topic of investigations for many years. In a series of works devoted to that topic it has been shown generally, that the liquid jet issuing from a small hole or a nozzle does not preserve its initial form and in effect breaks up into separate droplets, and the character of breakdown depends primarily of the liquid velocity, physical parameters of jet as well as the ambient gas. Such investigations have usually been conducted for the case of water jets flowing into the ambient air. On the basis of these experiments the liquid jet breakup phenomena have been divided into regimes that reflect differences in the appearance of jets as the operating conditions are changed. Generally speaking the liquid jets break up due to the disturbances imposed on the primary motion. The disturbances are in the form of axially-symmetric waves, asymmetric waves and more complex form induced by aero-dynamical forces.

The first form can be found at small efflux velocities. The jet breakdown occurs due to the influence of axially symmetric waves, which render appearance of the troughs on the jet. Due to the action of surface tension forces liquid is pumped from the troughs to the crests, which finally leads to the jet breakup and occurrence of droplet flow.

At higher efflux velocities, the jet axis is deformed and asymmetric waves are then formed. At even higher jet velocities the aero-dynamical forces, between surrounding gas and the jet surface, determine the breakdown.

These phenomena have been firstly investigated by Rayleigh [5], who explained the mechanism of jets instability. Weber [6] extended significantly the Rayleigh analysis. In the 30-ties of the twentieth century a lot of work was done on jets instability focused on the improvement of supply systems of direct injection engines (Diesel engines). These problems are widely discussed for example in the papers by Orzechowski [7-8].

It worth to note, that when dealing with the problem of jets instability very important role plays the measurement technique, particularly with the view of accurate determination of the lengths of the continuous liquid core, which represents the jet breakup length. At high efflux velocities the liquid core is surrounded by a slightly divergent cone consisting of small droplets [9-10]. Using the shadow photographic method with very short exposure times the cone gives on the photograph paper such a dense shadow, that the accurate determination of the core of the flow is almost impossible. For that reason, in the investigations of the liquid core length, a method based on electrical conductivity measurement has been used. Such method enables to determine more precisely the border between the both distinct flow patterns: the continuous liquid core structure and the dispersed gas-droplet flow.

The present paper concerns the complex investigations of the instability of water jets issuing from the contoured nozzles into stagnant air. This kind of nozzles are widely used in two-phase water-air ejectors as well as in the technology of free jets applied to surface cooling, surface cleaning, etc. The main goal of the investigations is to obtain a wide background on the jet structures as well as the relations of the jet breakup length in the function of the pertinent parameters. The data have been obtained using a modified very precise electric conductivity method. Owing to this method, the existence of a transition region between the liquid core and the droplet flow structures has been recognized.

2 Test rig

A schematic of the experimental rig constructed at IFFM PAS laboratory in order to conduct the investigation on the liquid jet instability, is presented in Fig. 1. The rig consists of the following major components: exchangeable contoured nozzle (2), water tank (7) and system of two feeding pumps (8). Water was pumped from the main tank (7) by means of two pumps (8), connected in series, to the nozzle (2). Pressure of the supplied water varied at the nozzle inlet in the range from 108 to 900 kPa (abs) accordingly to the nozzle diameter. The rig was also equipped with

- a measurement system of water volumetric flow rate (10) and the pressure measurement (11) as well as temperature measurement (12) systems,

- optical system for recording the jet structures (6),
- jet breakup length measurement system (13).

The elements of the test rig together with the measurement systems used are described in more detail in [11].

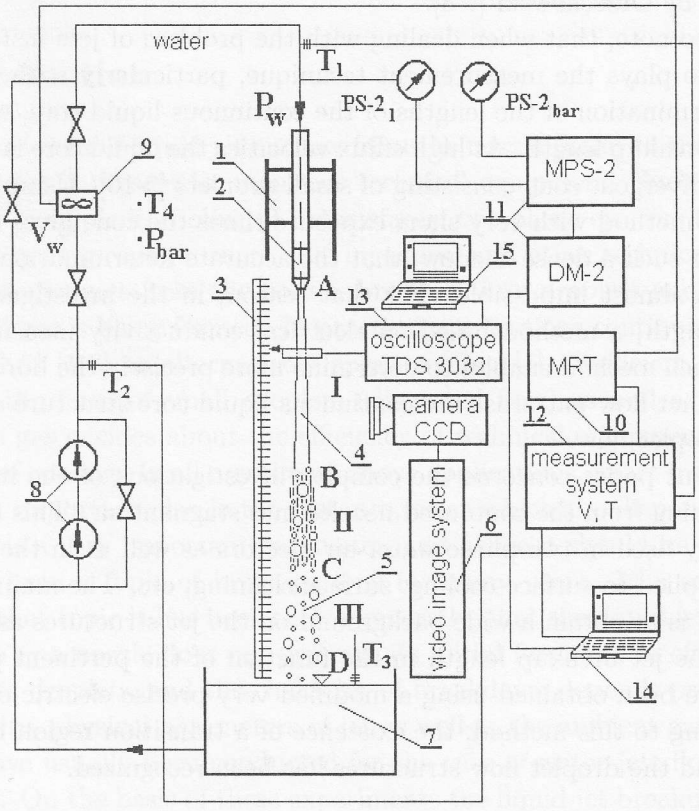

Figure 1. Schematic of the experimental rig for investigations of liquid jets structure: 1 – nozzle support, 2 – nozzle, 3 – measurement scale, 4 – liquid jet core region (region I), 5 – gas-droplet region (region III), 6 – video image system, 7 – main tank, 8 – set of pumps, 9 – turbine flow meter, 10 – measurement system of volumetric water flow rate, 11– pressure measurement system, 12 – measurement of T, V quantities, 13 – jet breakup length measurement, 14,15 – laptops, T – thermocouples.

3 Research methodology

The investigations of stability of liquid jets have been conducted using the contoured nozzles. Measurements have been done for three different nozzle outlet diameters: $D = 3.5$ mm, 6.0 mm and 9.5 mm. The shape and dimensions of

investigated nozzles are presented in Fig. 2.

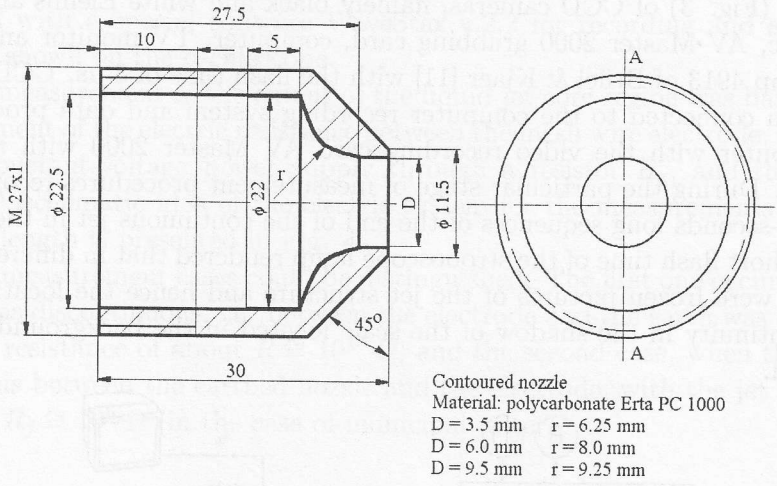

Figure 2. Shape and dimensions of the nozzle used in the experiments.

The research procedure involved the identification of the flow structures as well as the measurement of their extent. Owing to the measurement method used it was possible to identify the existence of three distinct regions in the jet flow. In connection to Fig. 1 we can talk about the existence of the following regions

- liquid jet core region – region I (segment AB in Fig. 1),
- transition region – region II (segment BC),
- dispersed flow region – region III (air-droplet flow – segment CD).

The following quantities have been measured during the investigations [11]

- water pressure in the nozzle,
- atmospheric pressure,
- water temperature,
- water flow rate in the jet,
- the extent of the particular regions I, II and III. These measurements have been conducted using a modified resistance method [11].

For the identification of the above regions a special optical system has been also used [11].

3.1 Optical system

The optical system for recording and identification of jet flow regions [11] consisted (Fig. 3) of CCD cameras, namely black and white Elemis and Colour Panasonic, AV Master 2000 grabbing card, computer, TV monitor and stroboscope lamp 4913 of Brüel & Kjaer [11] with the flash time of 3 μs. CCD cameras have been connected to the computer recording system and data processing (a PC computer with the video recording card AV Master 2000 with additional monitor). During the particular stage of measurement procedures recorded have been two-seconds long sequences of the end of the continuous jet in the AVI format. A short flash time of the stroboscope lamp rendered that in different frames recorded were frozen pictures of the jet structure and hence the location of the jet discontinuity in the shadow of the scale located in the background could be examined.

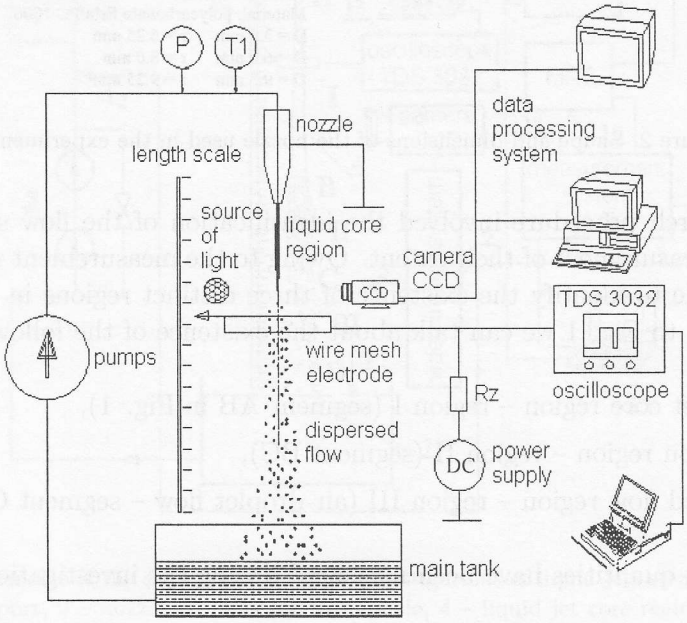

Figure 3. A schematic of the measurement system for identification of flow structure regions.

3.2 Measurement of the extent of the flow structures

The measurement system for the determination of the extent of flow regions I and II consisted of a metal mesh wire electrode spread over a rigid frame located in the plane normal to the nozzle axis (Fig. 3) and connected to 24 V DC power supply through a 1 MΩ resistor. The nozzle was earthed. The liquid jet flowing out the nozzle impinged on the mesh electrode. The position of the electrode

with respect to the nozzle exit was measured by using a length scale. The mesh electrode has been connected to the computer through the digital oscilloscope Tektronix TDS 3032 to display the electric signals. The computer has been equipped with a special software WaveStar v.2.2 for recording and acquisition the data shown on the oscilloscope.

The measurement of the extent of the liquid jet core region was based on the measurement of the electric resistance between the mesh wire electrode, connected to the constant-voltage power supply through a resistor R_z, and the earthed nozzle. A schematic idea of the electric system for the measurements of the jet breakup length is presented in Fig. 4.

Two measurement cases could be distinguished. The first one occurred, when the jet was discontinuous, i.e. between the electrode and the earth was an air gap with the resistance of about $R \cong 10^{10}\ \Omega$, and the second case, when the jet was continuous between the earthed nozzle and the electrode, with the jet resistance of about $R_j \cong 10^6\ \Omega$ (in the case of municipal water).

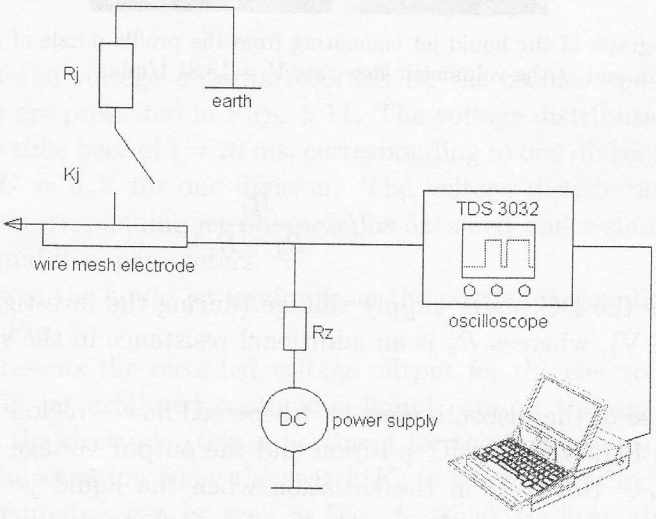

Figure 4. The principle of measurements of the extent of flow regions (structures) by means of the resistance method: R_j – jet resistance, R_z – additional resistance, K_j – virtual switch.

Assuming the liquid jet to be in the form of a cylinder of the length l and the diameter d then the value of the jet resistance R_j can be expressed as

$$R_j = \rho \frac{4l}{\pi d^2}, \tag{1}$$

where ρ is the specific resistance of water dependent on the chemical compositions and water temperature. The output voltage recorded by the oscilloscope is then

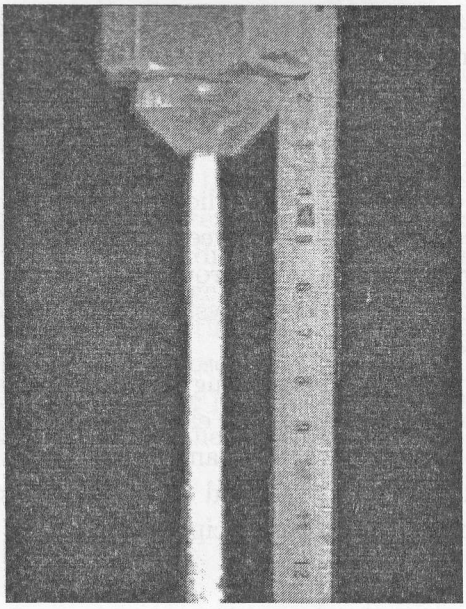

Figure 5. Photograph of the liquid jet emanating from the profile nozzle of the diameter $D = 3.5$ mm and at the volumetric flow rate $V = 13.81$ l/min.

equal to

$$U = U_{DC} \frac{R_j}{R_j + R_z}, \tag{2}$$

where U_{DC} is the DC power supply voltage (during the investigation it was set to $U_{DC} = 25$ V), whereas R_z is an additional resistance in the system shown in Fig. 4.

In the case of the discontinuous jet (dispersed flow – region III), the virtual switch K_j in Fig. 4 is in "off" position and the output voltage U is practically equal to U_{DC}. However, in the situation when the liquid jet appears in the continuous form (region I), the switch K_j is in "on" position. Then the output voltage U depends on the resistances R_j and R_z. The resistance R_z was selected in a such way that two characteristic measurement states: continuous liquid jet and the discontinuous one, could be distinguished. During the investigations of the extent of the flow regimes by means of the resistance method, the voltage output on the oscilloscope was approaching $U \cong 15$ V for the region I and $U \cong 25$ V for the region III. The distance from the nozzle exit to the locations which characterized the boundary between the first (I) and the second (II) regions, or between the second (II) and the third (III) ones were accomplished by mowing the electrode along the jet axis in order to achieve the required voltage outputs cited above.

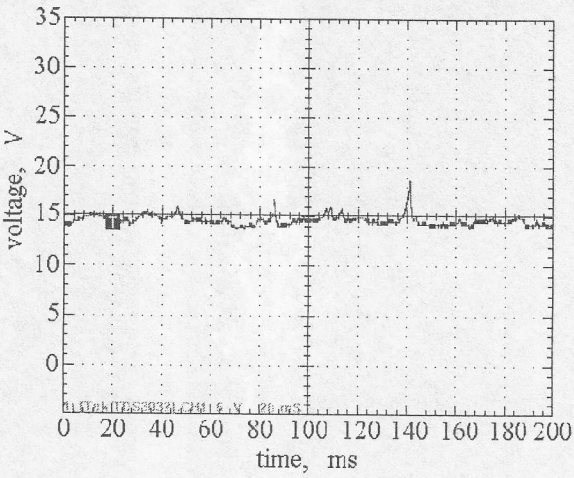

Figure 6. Voltage distribution on the oscilloscope for the electrode located at the border between I and II regions.

Samples of the voltage outputs recorded on the oscilloscope for the given flow conditions are presented in Figs. 5-11. The voltage distributions have been recorded at the time base of $t = 20$ ms, corresponding to one division, and voltage amplifying of $U = 5$ V for one division. The voltage distributions have been presented with corresponding jet photographs obtained under similar conditions at the same liquid flow parameters.

The picture of the liquid jet issuing from the nozzle for the above conditions is presented in Fig. 5.

Figure 6 presents the recorded voltage output for the electrode location at which the liquid jet exhibited continuous liquid core on the distance between the nozzle and the electrode (this is pertinent for the first region). Such case is equivalent to the situation when the switch K_j in the Fig. 4 is in "on" position. A few voltage impulses can be seen in Fig. 6, which confirm, that sometimes the continuity of the jet was broken. The voltage amplitude was about 5 V. The voltage output U in Fig. 6 was about 14 V, and hence the jet resistance R_j can be determined to be equal to 1.2 MΩ.

Such location of the electrode, when sometimes the jet discontinuity took place (but continuous liquid structure prevailed), determined in the present paper the border between the first and the second regions. The distance between the border and the nozzle exit describes thus the jet minimum breakup length $L_{b\,min}$ which is equal to $L_{b\,min} = L_I$.

Figure 7 presents the photograph for the same jet flow situation like in Fig. 5, but recorded in the place close to the mesh wire electrode. In the considered case,

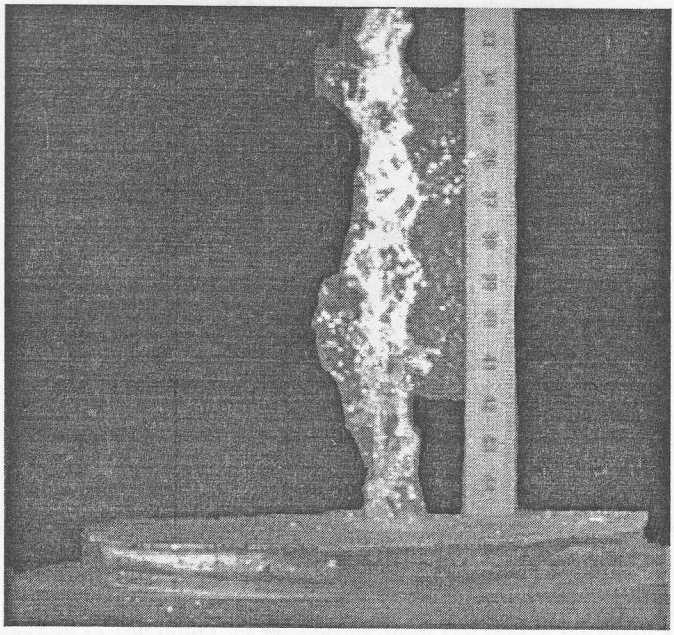

Figure 7. A photograph of the liquid jet in the neighbourhood of the electrode located at the border between I and II regions.

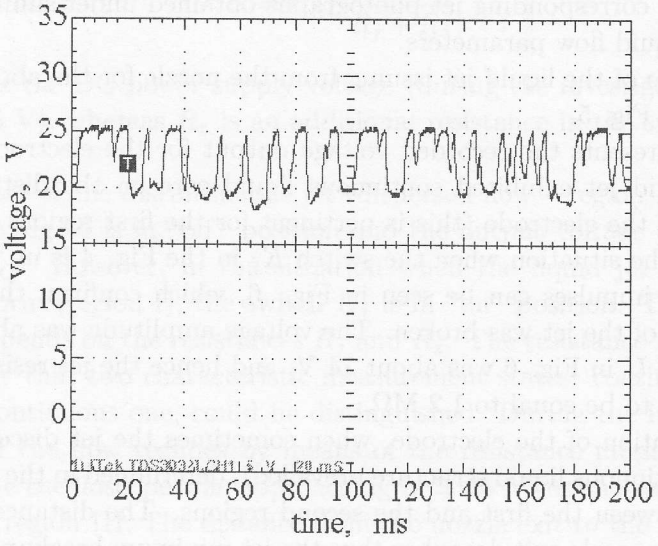

Figure 8. Distributions of the output voltage on the oscilloscope at the electrode located in the place where periodically the liquid jet core and the dispersed flow structures appeared.

the distance between the electrode location and the nozzle was established to be $L_{b\,min} = L_I = 38.6$ cm.

Figure 8 presents the voltage distribution on the oscilloscope for the electrode located in the transitional region II. Due to the random disturbances imposed on the primary jet flow, two flow structures may periodically occur in this region i.e.: liquid jet core and dispersed flow regimes. Both of them have equal probability to occur.

Referring to the Fig. 4 the appearance of the continuous liquid jet period is equivalent to the "on" position of the switch K_j and the existence of the dispersed flow i.e. the discontinuity periods is equivalent to "off" position of K_j. The discontinuity periods in that location varied in the range from 2 to 20 ms. The output voltage U in that case was equal to U_{DC} and had a value of 25V. For the case of appearance of continuous liquid jet between the nozzle and the electrode (switch K_j was in "on" position) the voltage output was about 18 V.

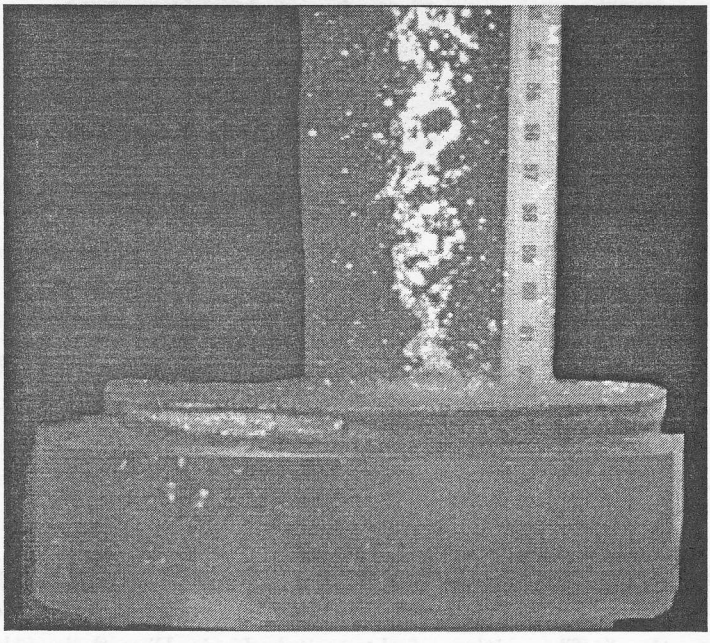

Figure 9. A photograph of the liquid flow situation corresponding to the case presented in Fig. 8 for the region II.

Figure 9 presents the jet photograph recorded in the neighbourhood of the electrode when the transition flow structure took place. It is seen that the jet lost it concise form pertinent for the liquid jet core region (see Fig. 5) and consist of liquid fiber-type ligaments. The occurrence of the liquid ligaments is a main feature of the second (transition) flow region.

The described case corresponded to the location of the electrode at the distance of $L_{II} = 62.2$ cm from the nozzle.

During the flow of liquid jet in the transition region the secondary breakup of the ligaments (liquid lumps) appears which finally leads to formation of small droplets embedded in the continuous gas phase. Thus fully developed dispersed flow structure (region III) is going to occur. However, before that, one shall think of a situation when occasionally the liquid lumps contact with one another what leads to "jet coalescence" and the reduction of the electrical resistance between the nozzle exit and the place of consideration. Thus it is seen that the flow structures in the transition region are unstable and periodically one structure prevails over the other.

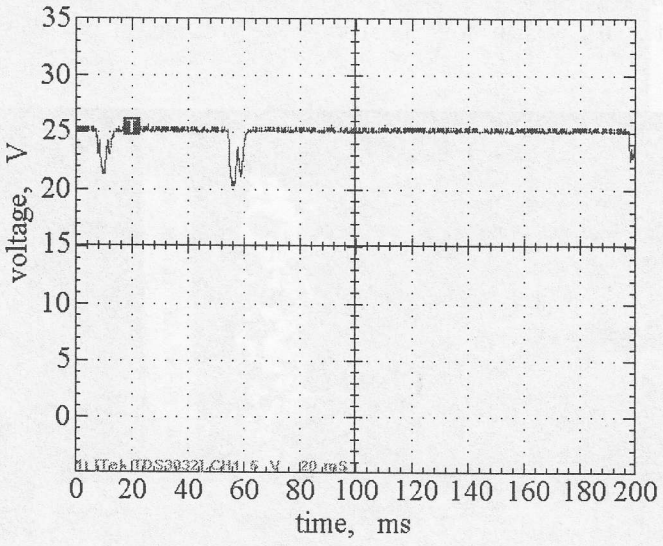

Figure 10. Voltage distribution on the oscilloscope for the electrode placed at the beginning of the flow region III.

The voltage signal on the oscilloscope at location of the electrode at the beginning of the region III is shown in Fig. 10. In that case voltage distribution corresponds to the "off" position of the switch K_j in Fig. 4, in other words it marks out the existence of the liquid jet physical discontinuity. Voltage base level U was equal to about 25 V. Two visible voltage impulses represent instances of time when the jet "coalescence" takes place, which appears as the voltage drop. Value of the voltage amplitudes varies from about 4 to 5V, and the voltage level during the "on" switch position (corresponding to a physical jet continuity) reaches 20 V. Such location of the electrode determines the end of the region II (transition), where the jet is periodically and very seldom continuous. At

the same location we may thus establish the beginning of the region III of fully developed dispersed flow. The distance between the beginning of the third flow region (III) and the nozzle exit determines the maximum jet breakup length $L_{iIII} = L_{b\ \max}$.

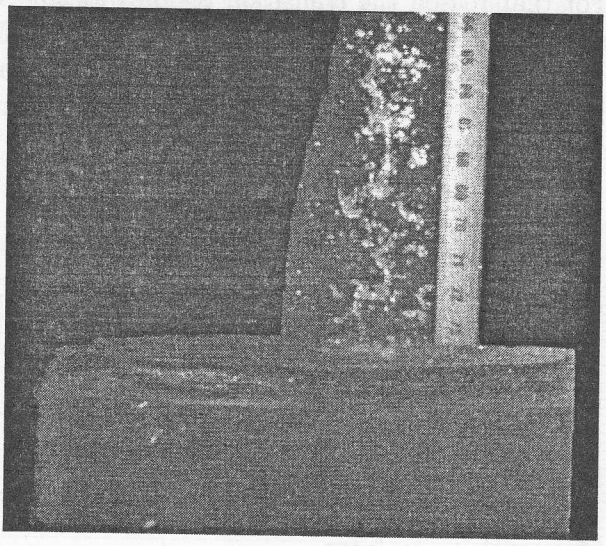

Figure 11. A photograph of the jet in the vicinity of the electrode placed at the beginning of the flow region III (Fig. 10).

Figure 11 presents a photograph of the jet recorded in the vicinity of the electrode. The distance between the electrode location and the nozzle was L_{iIII} = 73.7 cm. Taking into account the above considerations one may write that $L_{b\ \max} = L_{iIII}$ = 73.7 cm.

4 Experimental results

The details of the investigations of the instability of liquid jets issuing from contoured nozzles and the final results of breakup lengths L_I and L_{iIII} have been presented in [11]. Some of these results have also been shown in the Appendix in Fig. A1-A7, as well as in Tabs. 1-3 of the present paper.

It is an interesting issue how the our data of the liquid jet breakup lengths compare with data obtained by other authors. Fig. 12 presents the selected results of the jet breakdown length in the non-dimensional form L_b/D together with the data by other authors [12-13]. Based on the Fig. 12 it can be concluded

that investigations of those authors regarded only the length of the continuous jet $L_I = L_{b\,min}$, as the consistence between the authors own data and other experiments is satisfactory indeed. That issue is important for further comparisons, since in the relevant literature the phenomenon of the stability of liquid jets has been assumed as a step change from the continuous structure to the discontinuous one (droplets). For that reason the transition region was not considered, which apparently has a length of $L_{II} = L_{iIII} - L_I$. It can be seen from Fig. 12, that the maximum values of L_{iIII}/D are over 2.5 times greater than corresponding values of L_I/D in our data. Generally, the length of the transition region (II) is comparable in length with the continuous region length (I).

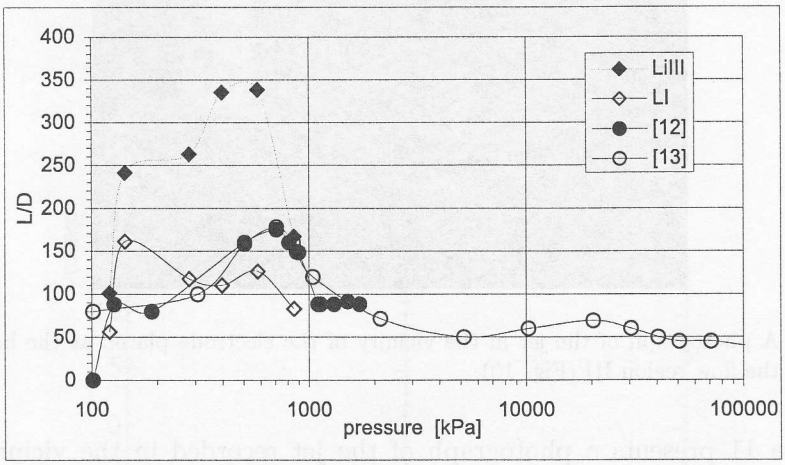

Figure 12. Distribution of non-dimensional lengths L_I/D and L_{iIII}/D in function of pressure for $D = 3.5$ mm nozzle.

For further discussion of the results it is worth presenting here the general form of jet breakdown length in a function of jet velocity at the nozzle outlet. That has been presented schematically in Fig. 13 based on the papers [14-15].

At small velocities ($w < w_m$), the length of a continuous part of the jet L_b increases with velocity. In the range of points between A and B it is a linear relation. Disturbances of the jet motion in the form of axially symmetric waves are responsible for the jet breakdown in the entire region AC. Next, with increasing velocity ($w > w_m$) the disturbances increase and the asymmetrical waves appear, [7]. These disturbances render that in the region CE there is observed a reduction of L_b. Next, at further increase of outflow velocity (the segment EF – broken line), there is a turbulisation of the jet leading consequently to the in-

crease of the length L_b. However, here a significant disturbance of motion can be found, which causes a sudden reduction of the jet length, curve EG. It is worth stressing, that in the vicinity of a point of maximum C in Fig. 13, there is present some plateau associated with the change of disturbance character. Generally, however, in the region AE of the breakdown curve the phenomenon is controlled by the surface tension forces and the reaction of surrounding. In the region EF and EG a dominant role is played by the inertia forces and forces of interaction between the jet and surrounding.

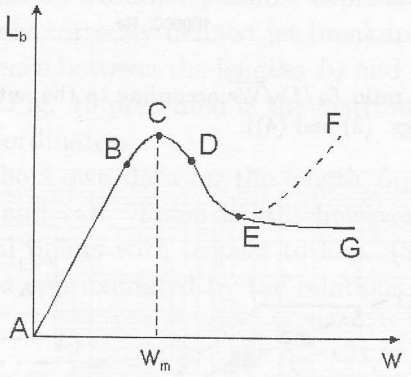

Figure 13. General shape of breakup curve [14].

The results of own investigations of the breakup length L_I in the first region is presented in Fig. 14 in adequately selected co-ordinates. Such a system of co-ordinates has been first suggested by Lienhard and Day [16], based on the theoretical considerations by Weber [6] with subsequent modifications by other authors.

Taking into account different investigations Lienhard and Day [16] proposed two correlations describing the jet breakdown length

$$\frac{L_b}{D\sqrt{\mathrm{We}}} = 2.75 \cdot 10^{10}\ \mathrm{Re}^{-2}, \tag{3}$$

for $\mathrm{Re} \geq 48000$
and

$$\frac{L_b}{D\sqrt{\mathrm{We}}} = 11.5 \tag{4}$$

for $\mathrm{Re} < 48000$.

Variation of breakup length L_b calculated according to Eqs. (3) and (4) have also been presented in Fig. 14.

Comparison between authors own data and Lienhard and Day Eqs. (3)

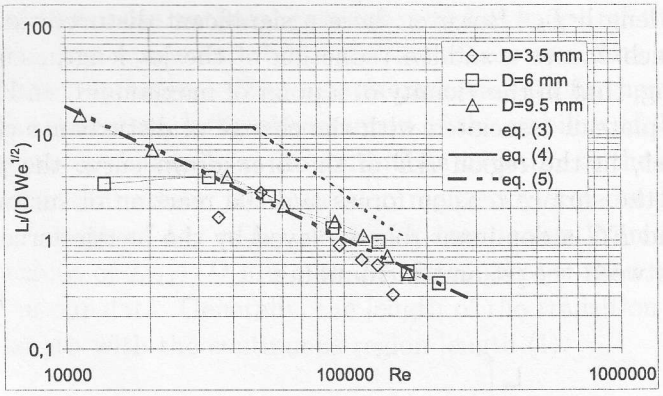

Figure 14. Variation of the ratio $L_I/D\sqrt{\mathrm{We}}$ according to the authors own data and Lienhard and Day [16] (Eqs. (3) and (4)).

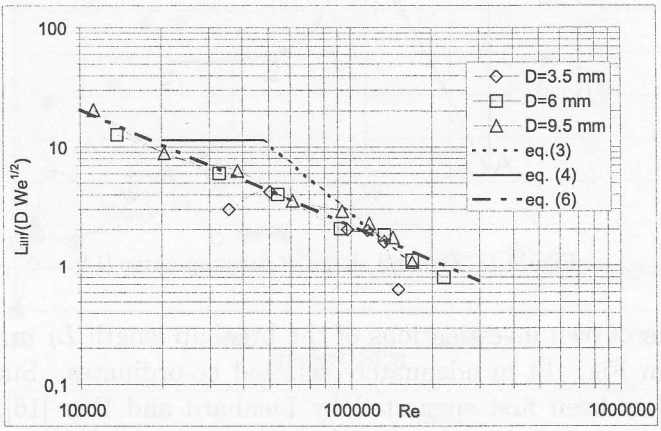

Figure 15. Variation of the ratio $L_{iII}/D\sqrt{\mathrm{We}}$ according to the authors own data and Lienhard and Day [16] (Eqs. (3) and (4)).

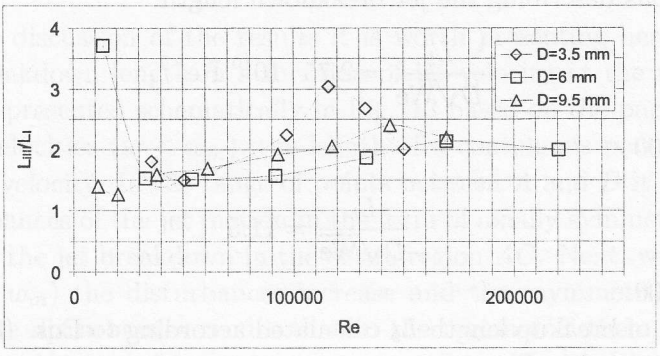

Figure 16. The ratio of the jet breakup lengths L_{iII}/L_I in the authors own investigations.

and (4) (regarded at present as the best ones) reveal that the authors own data are parallel shifted downward with respect to the latter. Authors own investigations are regarded the region CE from Fig. 13 since with the increase of the Reynolds number the breakup length L_I is decreasing. At smallest values of the Reynolds number (small jet velocities) there are however single deflections from the general trend with the direction described by Eq. (4) and hence characteristic to the region AC in the Fig. 13, when at the increase of velocity increases the jet breakdown length. At this moment it is rather difficult to explain the shift in data with respect to Lienhard and Day correlations. The reason can be hidden in other kind of used nozzles. Another possible explanation is that the authors of [16] used a not precisely correctly defined jet breakup length, hence were not accounting for the difference between the lengths L_I and L_{iIII}. In order to investigate the latter issue in Fig. 15 presented is the distribution of the length L_{iIII} in the same as above co-ordinates.

As expected the authors own data for the length L_{iIII} approached the data described by Eqs. (3) and (4). There is still however a difference as far as the slope of experimental points with respect to Eqs. (3) and (4) is concerned. Authors own data can be approximated by the relations

$$\frac{L_I}{D\sqrt{\mathrm{We}}} = 1.67 \cdot 10^6 \, \mathrm{Re}^{-1.24}, \tag{5}$$

for the region I (Fig. 14) and

$$\frac{L_{iIII}}{D\sqrt{\mathrm{We}}} = 1.74 \cdot 10^5 \, \mathrm{Re}^{-0.98}, \tag{6}$$

for the region III (Fig. 15), with the correlation coefficient $\mathrm{R}^2 = 0.97$ for both relations. The calculated values of L_I and L_{iIII} from the relations (5) and (6) respectively are also plotted in Fig. 14 and Fig. 15 for comparison.

The ratio of the lengths L_{iIII}/L_I is presented in the Fig. 16. It varies with the Reynolds number. As mentioned above its means value is about 2.

5 Concluding remarks

According to the present knowledge, the stability of laminar liquid jet issuing from the nozzle into stagnant gas is dependent primarily on the outflow velocity, initial motion disturbances, jet physical properties, parameters of the surrounding gas. Initial motion disturbances are amplified in the course of the flow and at some critical amplitude over the distance L_b there occurs the breakup of the jet continuity and appearance of a new form of the flow, namely the droplet flow. In such approach, the transition from the continuous form (liquid jet core region)

to the discontinuous form of the flow in the form of the droplet flow (dispersed flow) occurs abruptly and can be characterised by a physical discontinuity. The results presented in the paper contradict such opinion and clearly indicate on the transition between the both basic flow structures.

The work presents the results of investigations of instability of liquid jet emanating from the contoured nozzles into stagnant air. A computer-based optical system has been used for identification of liquid jet flow structures and owing to that fact several interesting results could be recorded. The precise measurement of the jet breakup lengths was possible due to the application of the electrical conductivity (or resistance) method after some modifications.

Based on the obtained results it has been shown, that the liquid jet flow region can be divided in respect to the liquid jet breakup length into three characteristic regions: continuous region (I) or liquid jet core region, transition region (II) and discontinuous region (stream of droplets – III). Existence of such pertinent regions enables to draw several important conclusions:

1. Transition region of the jet flow in respect to it instability falls between the regions I and III. Hence the length L_{II} of the jet in this region fulfils the inequality, $L_I \leq L_{II} \leq L_{iIII}$. The region II is characterized by the equal probability of occurrence of both: the liquid jet core and dispersed flow structures. In other words the liquid jet breakup lengths may change in the value described by the inequality, $L_I \leq L_b \leq L_{iIII}$.
2. Due to possible applications in jet cooling or surface cleaning using liquid jets, the maximum length of such jet should obey the condition, $L_{j\ \max} < L_I$.
3. In using of liquid jets in the form of droplets for spray cooling another inequality should be obeyed, $L_s > L_{iIII}$.
4. The length of the transition region, determined by the ratio L_{iIII}/L_I, is significant ($L_{iIII}/L_I \cong 2$) and is comparable with the length of the region I.
5. Omission of the existence of transition region in previous investigations, cited in the literature, can be one of two major reasons for the significant discrepancy of results in that area. An extensive survey of investigations of the stability of jets can be found, amongst the others, in [17]. A second important reason for the discrepancy in a series of investigations can be rendered by a different extent of the initial disturbance in the jet motion. Its magnitude is mainly dependent on the installation vibrations and the geometry of the nozzles.

Equations (5) and (6) proposed for determination of the characteristic jet lengths L_I and L_{iIII} are valid for the contoured nozzles (Fig. 2) in the following range of dimensionless numbers: $10000 < \mathrm{Re} < 220000$, $50 < \mathrm{We} < 47000$.

Received 20 February 2002

References

[1] Shih-Jiun Chen, Tseng A. A.: *Spray and jet cooling*, Int. J. Heat Fluid Flow, **13**(1992), 4, 358-369.

[2] Chen J., Kothari J., Tseng A.: *Cooling of moving plate by an impinging circular water jet*, Exp. Thermal Fluid Sci., **3**(1991), 343-353.

[3] Rymkiewicz J., Trela M.: *The radial spread of a free liquid jet over a horizontal cylinder*, Proc. Int. Symposium on *Heat Transfer and Renewable Energy Sources*, Szczecin-Łeba, 2000, 327-334.

[4] Bolle L., Monreau J. C.: *Experimental study of heat transfer by spray cooling*, Heat and Mass Transfer in Metallurgical Systems, Hemisphere, Washington, DC, 1981, 527-534.

[5] Rayleigh Lord : *On the instability of jets*, Proc. London Math. Soc. Vol. 10, 1879, 4-10.

[6] Weber C.: *Zum Zerfall eines Flüssigketsstrahles*, Z. Angew. Math. Mech. **11**(1931), 2, 136-154.

[7] Orzechowski Z.: *Liquid spraying*, WNT, Warszawa 1976.

[8] Orzechowski Z., Prywer J.: *Liquid spraying in power engineering equipment*, WNT, Warszawa 1994.

[9] Wereshchagin L. F., Semerchan A. A., Firsov A. I., Galaktyonov W. A., Filler F. M.: *Investigations of liquid jet flowing out the nozzle under pressure of 1500 at*, Zhurnal Tekhnicheskoy Fiziki, Vol. XXVI, wyp. 11, 1956, 2570-2577, (in Russian).

[10] Wereshchagin L. F., Semerchan A. A., Filler F. M.: *Investigations of liquid jet flowing out the nozzle under pressure of 2000 at*, Izviestiya Akademii Nauk SSSR, Otdelenye Tekhnicheskikh Nauk, **1**(1957), 57-60, (in Russian).

[11] Ihnatowicz E., Krupa A., Trela M.: *Influence of the feeding nozzle and its diameter on the jet breakup*, IFFM PAS Internal Report, nr 1720/2001, Gdańsk, 2001.

[12] Pazhi D. G., Galustov W. S.: *Fundamentals of liquid spraying*, Khimiya, Moskva 1984, (in Russian).

[13] Wereshchagin L. F., Semerchan A. A., Sekoyan S. S.: .: *On the problem of high velocity water jet breakup*, Zhurnal Tekhnicheskoy Fiziki, Vol. XXIX, **1**(1959), 45-50, (in Russian).

[14] Grant R. L., Middleman S.: *Newtonian jet stability*, AIChE Journal, **12**(1966), 4, 1966.

[15] Middleman S.: *Modeling axisymmetric flows, dynamics of films, jets, and drops*, Academic Press, New York, London 1995.

[16] Lienhard J. H., Day J. B.: *The breakup of superheated liquid jets*, Trans. of the ASME, J. of Basic Engineering, September 1970, 515-522.

[17] Biń A. K.: *Gas entrainment by plunging liquid jets*, VDI Forschungsheft 648/1988, 1-36.

Appendix

The experimental data shown below concern the jet breakup lengths for the three diameters of the contoured nozzles. Figs. A1, A3, A5 present the lengths L_I and L_{iIII} of water jet flowing out the nozzles with diameters 3.5 mm, 6 mm and 9.5 mm, respectively, in function of volumetric flow rate of water. On the other hand, in Figs. A2, A4, A6 given are the lengths of water jets L_I and L_{iIII} in function of water pressure in the nozzle for corresponding nozzle diameters as above.

Figure A7 presents an overall variations of the breakup lengths L_I and L_{iIII} for water jets flowing out the nozzles with diameters: 3.5 mm, 6.0 mm and 9.5 mm at varying pressure in the nozzles.

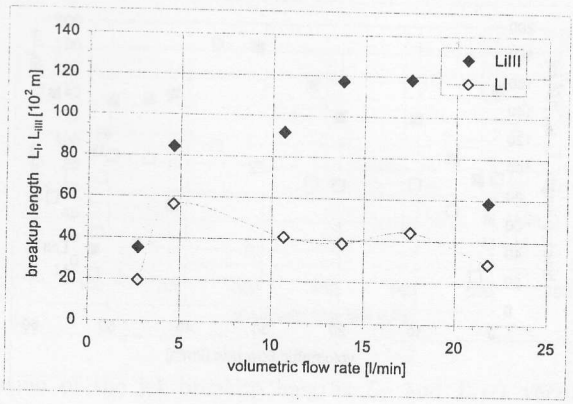

Figure A1. Variation of the jet breakup lengths L_I and L_{iIII} versus the flow rate for $D = 3.5$ mm nozzle.

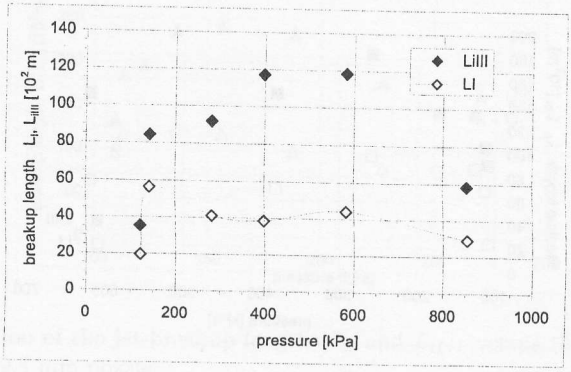

Figure A2. Variation of the jet breakup lengths L_I and L_{iIII} versus the water pressure for $D = 3.5$ mm nozzle.

Table 1. Results of measurements for the nozzle with diameter $D = 3.5$mm

Lp.	T1	T2	T3 tank	T4 air	V_w	$L_I \cdot 10^2$	$L_{iIII} \cdot 10^2$	P_w	P_{bar}
	$[^oC]$	$[^oC]$	$[^oC]$	$[^oC]$	[l/min]	[m]	[m]	[kPa]	[kPa]
1	63.17	61.51	25	23.2	2.71	19.7	35.4	120.8	99.26
2	50.72	49.69	25.1	23.2	4.62	56.4	84.4	142.4	99.26
3	39.95	39.49	25.2	23.6	10.64	41.2	92	281.3	99.26
4	35.38	35.09	24.4	23.6	13.81	38.6	117.3	398.3	100.9
5	30.35	30.15	22.3	23.6	17.51	44.2	118.4	582.4	100.9
6	25.83	25.79	22	23.6	21.77	29.1	58.5	853.9	100.9

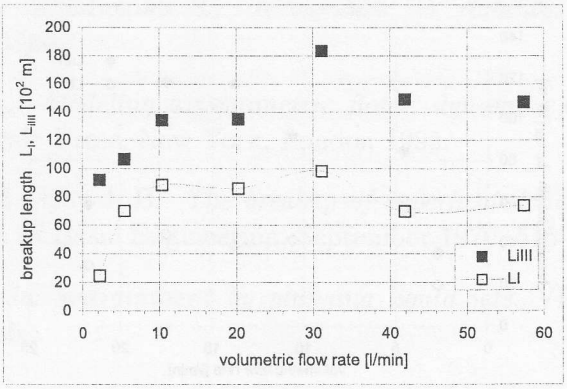

Figure A3. Variation of the jet breakup lengths L_I and L_{iIII} versus the flow rate for $D = 6$ mm nozzle.

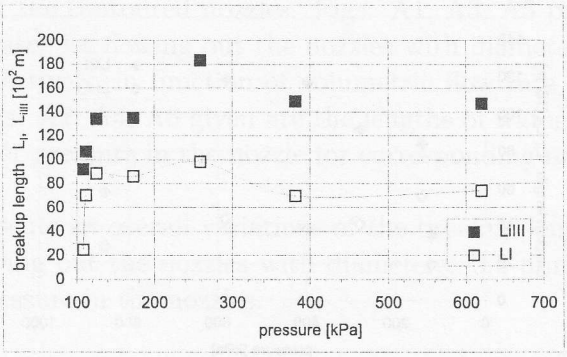

Figure A4. Variation of the jet breakup lengths L_I and L_{iIII} versus the water pressure for $D = 6$ mm nozzle.

Table 2. Results of measurements for the nozzle with diameter $D = 6.0$ mm

Lp.	T1	T2	T3 tank	T4 air	V_w	$L_I \cdot 10^2$	$L_{iIII} \cdot 10^2$	P_w	P_{bar}
	$[^oC]$	$[^oC]$	$[^oC]$	$[^oC]$	[l/min]	[m]	[m]	[kPa]	[kPa]
1	51.76	48.42	24.8	21.1	2.2	24.8	92	108.6	100.6
2	47.13	46.66	25.2	21.1	5.42	70.2	106.9	112.5	100.4
3	38.84	38.33	26.3	21.1	10.34	88.5	134.3	125.7	100.4
4	31.63	31.18	23.7	21.1	20.24	86.1	135	172.9	100.4
5	28.32	28.53	23.7	21.1	31.11	98.3	183.3	258.9	100.4
6	26.39	25.92	22	21.1	41.92	69.8	148.1	381	100.4

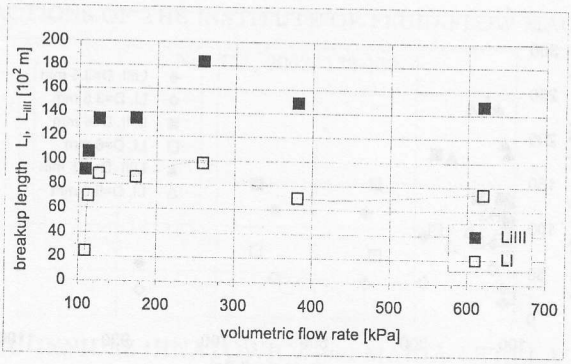

Figure A5. Variation of the jet breakup lengths L_I and L_{iIII} versus the flow rate for $D = 9.5$ mm nozzle.

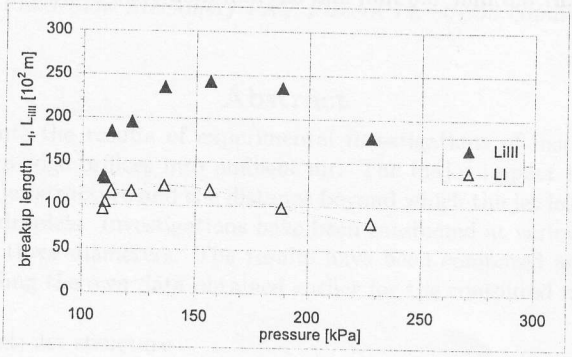

Figure A6. Variation of the jet breakup lengths L_I and L_{iIII} versus the water pressure for $D = 9.5$ mm nozzle.

Table 3. Results of measurements for the nozzle with diameter $D = 9.5$ mm

Lp.	T1	T2 [°C]	T3 tank	T4 air	V_w	$L_I \cdot 10^2$	$L_{iIII} \cdot 10^2$	P_w	P_{bar}
	[°C]	[°C]	[°C]	[°C]	[l/min]	[m]	[m]	[kPa]	[kPa]
1	61.67	58.33	28	24.1	2.44	95.4	132.8	109.1	101.7
2	44.62	43.68	27.5	24.1	5.64	103.4	130.4	110	101.7
3	39.72	39.78	26.9	24.1	11.26	116.4	184.4	112.7	101.7
4	31.58	31.48	26.2	24.1	21.27	115.9	195.4	121.6	101.7
5	32.4	32.77	27.3	24.1	31.51	122.5	235.4	136.1	101.7
6	30.96	31.07	27	24.1	41.26	118.2	242.5	156.2	101.7
7	28.36	28.48	25.6	24.1	53.31	98.2	235.4	188.2	101.8
8	26.55	26.33	22.8	24.1	65.75	81.7	179.4	227.6	101.8

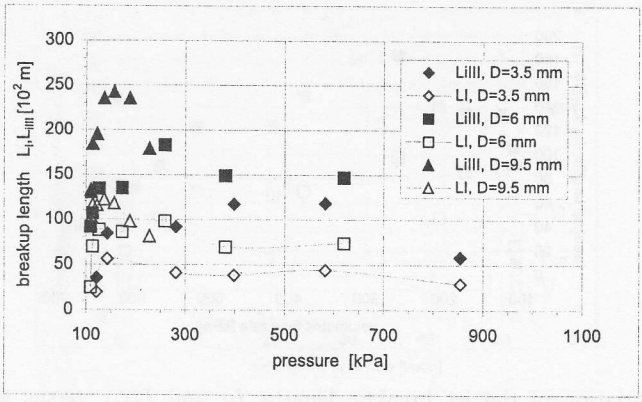

Figure A7. Variation of the breakup lengths L_I and L_{iIII} versus the nozzle water pressure for: 3.5 mm, 6.0 mm and 9.5 mm diameters nozzles.